THE JOURNAL OF BIOLOGICAL CHEMISTRY VOL. 285, NO. 45, pp. 34909–34921, November 5, 2010

Regulation of Epidermal Growth Factor Receptor Ubiquitination and Trafficking by the USP8·STAM Complex*[S]

Received for publication, May 2, 2009, and in revised form, August 2, 2010 Published, JBC Papers in Press, August 24, 2010, DOI 10.1074/jbc.M109.016287

Ilana Berlin[1], **Heather Schwartz, and Piers D. Nash**[2]

From the Ben May Department for Cancer Research, The University of Chicago, Chicago, Illinois 60637

Reversible ubiquitination of activated receptor complexes signals their sorting between recycling and degradation and thereby dictates receptor fate. The deubiquitinating enzyme ubiquitin-specific protease 8 (USP8/UBPy) has been previously implicated in the regulation of the epidermal growth factor receptor (EGFR); however, the molecular mechanisms governing its recruitment and activity in this context remain unclear. Herein, we investigate the role of USP8 in countering ligand-induced ubiquitination and down-regulation of EGFR and characterize a subset of protein-protein interaction determinants critical for this function. USP8 depletion accelerates receptor turnover, whereas loss of hepatocyte growth factor-regulated substrate (Hrs) rescues this phenotype, indicating that USP8 protects EGFR from degradation via an Hrs-dependent pathway. Catalytic inactivation of USP8 incurs EGFR hyperubiquitination and promotes receptor localization to endosomes marked by high ubiquitin content. These phenotypes require the central region of USP8, containing three extended Arg-*X*-*X*-Lys (R*XX*K) motifs that specify direct low affinity interactions with the SH3 domain(s) of ESCRT-0 proteins, STAM1/2. The USP8·STAM complex critically impinges on receptor ubiquitination status and modulates ubiquitin dynamics on EGFR-positive endosomes. Consequently, USP8-mediated deubiquitination slows progression of EGFR past the early-to-recycling endosome circuit in a manner dependent upon the R*XX*K motifs. Collectively, these findings demonstrate a role for the USP8·STAM complex as a protective mechanism regulating early endosomal sorting of EGFR between pathways destined for lysosomal degradation and recycling.

Endocytosis of growth factor receptors in response to ligand engagement mediates signal attenuation through selective targeting of activated receptor complexes for lysosomal proteolysis (1). Reversible ubiquitination, orchestrated by the opposition of ubiquitin ligases and deubiquitinating enzymes (DUBs)[3] (2), specifies sorting of endocytosed cargo (3, 4), with mono-ubiquitination and lysine 63-linked polyubiquitination extensively documented to promote trafficking of EGFR to the preproteolytic multivesicular body (MVB) compartment (5–7). Four functionally distinct endosomal sorting complexes required for transport (ESCRTs 0, I, II and III) are known to be involved in the coordinated selection, commitment, and delivery of ubiquitinated cargo for lysosomal degradation (8). The ESCRT-0 complex, consisting of adaptor proteins hepatocyte growth factor-regulated substrate (Hrs) and signal transducing adaptor molecule (STAM) (9), partitions cargo arriving at the sorting endosome between recycling and progression to the MVB (10–13) and, thus, constitutes a critical regulatory checkpoint in the determination of receptor fate.

Complexity and selectivity of receptor trafficking is modulated by reversible ubiquitination of receptors as well as components of endocytic sorting machinery (8, 14–16). Increasing evidence suggests that ubiquitin ligases and DUBs associate with the ESCRT proteins to modulate trafficking outcomes. Specifically, the yeast ESCRT-0 complex, composed of the Hrs and STAM orthologs Vps27 and Hse1, respectively, interacts with the ligase Rsp5 and the DUBs Ubp2 and Ubp7 to allow cargo sorting into the MVB (17). Similarly, deficiencies in Hrs and STAM proteins impair EGFR trafficking and degradation and lead to gross endocytic swelling, characteristic of defects in cargo progression (11). A high degree of structural conservation between the yeast and human ESCRT-0 complexes (18) implies functional and regulatory similarities. In support of this notion, the mammalian STAM1/2 proteins have been shown to interact *in vitro* with two DUBs: USP8 and the associated molecule with the SH3 domain of STAM (AMSH) (19–22).

An essential growth-regulated enzyme, USP8, is indispensable to cellular proliferation and survival (23, 24). Analysis of a conditional USP8 mouse knock-out has revealed a drastic loss of growth factor receptors, including the EGFR, its family member, Erb-B3, and c-Met (24). These phenotypes are further accompanied by accumulation of ubiquitinated species at the early-to-late endosome transition as well as endosomal swelling akin to inhibition of Hrs (25). Consistent with these findings, USP8 inactivation leads to enhanced ubiquitination of EGFR in response to ligand-induced activation (26, 27), and USP8 phosphorylation on serine 680 during M-phase results in 14-3-3 binding and reduced receptor deubiquitination (28).

* This work was supported by the American Cancer Society, Illinois Division, the Concern Foundation, and the V Foundation Scholars Program (to P. D. N.).
[S] The on-line version of this article (available at http://www.jbc.org) contains supplemental Figs. S1–S4.
[1] Recipient of a Department of Defense (Congressionally Directed Medical Research Programs) Breast Cancer pre-doctoral fellowship.
[2] To whom correspondence should be addressed: 929 East 57th St. W432, Chicago, IL 60637. E-mail: pdnash@uchicago.edu.
[3] The abbreviations used are: DUB, deubiquitinating enzyme; EGFR, EGF receptor; MVB, multivesicular body; ESCRT, endosomal sorting complexes required for transport; Hrs, hepatocyte growth factor-regulated substrate; STAM, signal transducing adaptor molecule; AMSH, associated molecule with the SH3 domain of STAM; USP8, ubiquitin-specific protease 8; MIT, microtubule interacting and transport; Rhod, rhodanese-like domain; IF, immunofluorescence; BiFC, bimolecular fluorescence complementation; VFP, venus fluorescent protein; USP, ubiquitin-specific peptidase; *WCL*, whole cell lysate; IP, immunoprecipitate; Fl, fluorescein.

Collectively, published evidence demonstrates a requirement for USP8 in EGFR stabilization against lysosomal turnover and implicates USP8 as a positive regulator of the early sorting machinery (24, 29) indispensible for receptor trafficking. Because trafficking of EGFR for degradation proceeds through an Hrs-dependent pathway (11, 30, 31), recruitment of USP8 to the ESCRT-0 complex may critically impinge on early sorting events and, thus, influence receptor fate. Despite recent progress, the molecular determinants responsible for targeting USP8 activity to these proteins *in vivo* remain poorly understood.

Although a number of protein-protein interaction domains and motifs in USP8 have been identified, their contributions to the regulation of EGFR are unclear. The N-terminal domain of unknown function (DUF) 1873 of USP8 reportedly constitutes a structurally atypical low homology microtubule interacting and transport (MIT) domain (32, 33), which has been shown to interact *in vitro* with the CHMP-1A/B protein components of the late endosomal sorting complex, ESCRT-III. Consistent with this characterization, cellular distribution of USP8 has been reported to straddle the endosomal continuum between the early and late extremes (27, 34, 35), and USP8 activity has previously been implicated at the late endosome stage (35). Nevertheless, consequences of such an association between USP8 and the ESCRT-III complex with regard to EGFR ubiquitination (the determinate signal in receptor trafficking known to be directly modulated by USP8) have not been addressed. In addition, the rhodanese-like domain (Rhod) of USP8 is known to bind the E3 ligase, Nrdp1, and in so doing indirectly influences the degradation of Erb-B3 (33, 36, 37). A truncation of USP8 containing both MIT and Rhod has been shown to interact with activated EGFR complexes (26); however, the extent to which these domains participate in the regulation of EGFR ubiquitination and trafficking by USP8 is unclear.

In a mammalian library screen of binding targets for non-canonical SH3 domains found in proteins belonging to the STAM and Grb2 families, two consensus P*X*(V/I)(D/N)R*XX*KP (R*XX*K) motifs of USP8 have previously been identified (19). Although the existence of a functional relationship between USP8 and the ESCRT-0 proteins has been hypothesized on that basis (24, 25, 29), no direct link between receptor endocytosis and the R*XX*K-mediated recruitment of USP8 to STAM has been described. To evaluate this premise, the present study (*a*) characterizes the USP8 sequence determinants necessary and sufficient to support an interaction with the SH3 domains of STAM1/2 and (*b*) explores the role of the USP8·STAM complex in mitigating EGFR ubiquitination and downstream trafficking events. We find that USP8 depletion accelerates ligand-induced degradation of EGFR through a pathway regulated by Hrs and describe three low affinity R*XX*K motifs responsible for the interaction with the Hrs partner, STAM. The USP8·STAM complex impinges upon the ESCRT-0 ubiquitination status and modulates ubiquitin dynamics on EGFR-positive endosomes. Furthermore, mutational analysis reveals that USP8 acts to constrain EGFR ubiquitination in a manner dependent upon the R*XX*K motifs of USP8, with no contribution to this function observed for the MIT domain. Finally, we demonstrate a role for the R*XX*K-mediated interactions in receptor trafficking downstream of the ubiquitination event opposed by USP8 activity. Our results, therefore, illustrate a functional cooperation between USP8 and ESCRT-0 proteins in the regulation of dynamic ubiquitin-dependent events in growth factor receptor endocytosis.

MATERIALS AND METHODS

Mammalian Expression Constructs and Recombinant Protein Expression—Mammalian expression constructs of murine USP8 (BC50947), ubiquitin, STAM1 (BC044666), STAM2 (BC013818), and Gads (BC052496) were cloned by PCR into the pcDNA3.1 (+) vector system (Invitrogen) at BamHI/EcoRI. N-terminal FLAG, Myc, or HA epitope tags were inserted at the BamHI restriction site using annealed primer pairs or introduced at the 5′ end of forward PCR primers. For the BiFC assay, USP8 and mutants were cloned by PCR into pBiFC-VN173-FLAG vector at NotI/EcoRI, and murine STAM1, STAM2, and Grb2 (BC052377) were cloned into pBiFC-VC155-HA vector at EcoRI/XhoI. HA-CXCR4 construct in pcDNA3.1 (38) and BiFC expression vectors have been previously described (39). Site-directed mutagenesis of USP8 to generate the C748A and R3K mutants (R409K, R438K, and R704K) as well as the SH3 domain mutants of STAM1-WA (W287A), STAM2-EEAA (E217A, E220A), and Gads-WA (W300A) was performed using QuikChange PCR (Stratagene). All PCR primers were purchased from Integrated DNA Technologies. The GST fusion SH3 domain constructs as well as fragments of USP8 and Slp76 (BC016618) containing the R*XX*K motifs were generated by PCR cloning into pGEX-2TK (Invitrogen) vector system at BamHI/EcoRI. Expression and purification of GST fusion proteins were carried out as previously described (19).

Cell Lines, Transfection, and siRNA—HeLa cells were used for all experiments requiring cell cultures in this study. Cells were grown in DMEM (CellGrow) and supplemented with 10% FBS (Sigma). All transfections were performed using Lipofectamine 2000 (Invitrogen). Transient knockdown was accomplished either through direct transfection of siRNA oligonucleotides or expression of pSilencer vectors to generate siRNA. Ambion oligonucleotide 105117 targeted against USP8 (siUSP8) and Silencer Negative Control #1 were obtained from Applied Biosystems. pSilencer vector and negative control were purchased from Ambion. A previously reported sequence (27) coding an anti-USP8 siRNA was custom-synthesized by Integrated DNA Technologies and cloned into the pSilencer vector according to the manufacturer's instructions. Two previously published siRNA sequences targeting human Hrs were used; siHrs-2 (38) was custom synthesized by Applied Biosystems, and results were verified using siHrs-1 sequence purchased from Dharmacon (31).

Western Blotting and Antibodies—The following primary mouse monoclonal antibodies were used for Western blotting and immunofluorescence (IF): anti-β-actin and anti-FLAG 3165 (Sigma), anti-CD63 (Developmental Studies Hybridoma Bank, The University of Iowa), anti-EGFR F4 (Santa Cruz), anti-HA (Covance), anti-Myc and anti-phosphotyrosine (CST or Santa Cruz), and anti-transferrin receptor (Invitrogen). The following primary rabbit polyclonal antibodies were used: anti-

EGFR (Upstate), anti-FLAG (Stratagene), anti-HA (Sigma), and anti-STAM1 (Calbiochem or Santa Cruz). Rabbit USP8 and Hrs antisera were generated against GST fusion proteins of murine USP8 corresponding to amino acid residues 1–184 (anti-USP8*), amino acid residues 393–432 (anti-hUSP8), and murine Hrs (BC003239) amino acid residues 216–289. Polyclonal goat anti-GST was purchased from Amersham Biosciences. Goat secondary antibodies anti-mouse AlexaFluor-800 and anti-rabbit-AlexaFluor-680 for Western blotting were purchased from LI-COR. Goat secondary antibody anti-rabbit and anti-mouse AlexaFluor-488/568/647 conjugates for IF were purchased from Molecular Probes. All Western blots were visualized with LI-COR Odyssey infrared imager, and band intensities were quantified using Odyssey 3.0 software. Final image processing was performed in Adobe Photoshop CS3 and was limited to brightness enhancement and cropping. All graphical representations were generated using DeltaGraph7.5.5 software.

Degradation Assays—To measure the rate of EGFR degradation, cells were transfected with either control or anti-USP8 siRNA oligonucleotides at a final concentration of 50 nM or pSilencer vectors containing either a control insert sequence (Ambion) or an insert targeting human USP8 (27). After transfection, cells were grown for 48 h, serum-starved in DMEM supplemented with 0.1% FBS, and treated in the presence of 2.5 ng/ml EGF for the specified length of time, and changes in the total cellular EGFR observed throughout the treatment time course were assessed by Western blot against the endogenous receptor. Degradation plots were generated by fitting EGFR abundance measured at each treatment time point relative to unstimulated cells to: $EGFR_{relative} = EGFR_{flux}e^{-Rt} + EGFR_{stable}$ ($EGFR_{relative}$, EGFR abundance relative to t_0 (time = 0 min); $EGFR_{flux}$, 82% of total cellular EGFR (amount of receptor determined to be susceptible to EGF-mediated degradation); R, rate constant; t, time of stimulation with EGF; $EGFR_{stable}$, 18% of total cellular EGFR (amount of receptor determined to be unaffected by degradation in response to EGF)). In experiments combining USP8 and Hrs knockdown, cells were transfected with 50 nM total concentration of oligonucleotides and treated as above. Receptor turnover was reported as % of receptor degraded during the time of treatment relative to $t = 0$ min.

Ubiquitination Assays—HeLa cells were seeded at 7.5×10^5 per 60-mm tissue culture plate and allowed to adhere overnight. Cells were co-transfected with 1 μg of HA-ubiquitin and 2 μg of other DNA or 50 nM siRNA as specified. For EGFR ubiquitination analysis, 24-h post-transfection cells were serum-starved for 4 h and treated with 2.5 (with USP8 depletion) or 10 ng/ml (with USP8·STAM overexpression) EGF (Roche Applied Science) as indicated for 5 or 10 min at 37 °C. After treatment, cells were washed with ice-cold PBS and lysed on ice in 300 μl of lysis buffer (50 mM Tris-HCl, pH 7.5, 150 mM NaCl, 0.5% Triton X-100, 10 mM NaF, 1 mM Na_3VO_4, 1 mM PMSF, protease inhibitors mixture (Roche Applied Science)). Lysates were clarified at 10,000 rpm at 4 °C and incubated with 150 μl of TBS containing 0.1% Tween (TBST), 3 μg of anti-EGFR 528 antibody (Santa Cruz), and ProteinG beads (Roche Applied Science) rotating at 4 °C overnight. Beads were then washed 3× with 0.75 ml of ice-cold TBST and eluted in 2×S DS gel loading buffer supplemented with 200 mM dithiothreitol (DTT). Samples were subjected to 8% SDS-PAGE and transferred onto nitrocellulose membranes, and ubiquitination was assayed by Western blot against HA-ubiquitin.

Immunofluorescence Microscopy—For co-localization of EGFR with intracellular ubiquitin as a function of USP8 activity (see Fig. 2*D*), HeLa cells were seeded at $2.5–3 \times 10^5$ per well onto polylysine-coated glass coverslips (Corning) in 6-well tissue culture plates and allowed to adhere overnight. Cells were transfected with USP8 or mutant DNA and HA-ubiquitin at 5:1 to ensure that cells overexpressing tagged ubiquitin also expressed exogenous USP8 protein. 8 h after transfection cells were briefly serum-starved (1 h) and treated in the presence of 10 ng/ml EGF for 10 min, fixed and permeabilized in 1:1 methanol:acetone solution for 20 min at −20 °C, and immunostained against HA-ubiquitin and endogenous EGFR (Upstate Biotechnology).

For IF using CFP overexpression, cells were seeded as above and transfected with CFP alone, USP8-CFP, or mutant for 24 h, briefly serum-starved, and treated in the presence of 10 ng/ml EGF for 10 min. Cells were fixed in 4% paraformaldehyde in PBS for 10–15 min at room temperature and stored at 4 °C before staining. Permeabilization with 0.1% Triton X-100 in PBS for 10–15 min was performed immediately before immunostaining. All immunostaining, except for anti-CD63 was carried out in 5% milk in PBS according to standard protocols. Coverslips were mounted onto glass slides using ProLong Gold antifade mounting media (Invitrogen). For immunostaining with anti-CD63, permeabilization and antibody incubations of cells fixed with paraformaldehyde were carried out in 3% BSA, PBS containing 0.05% saponin.

Samples were imaged on a Leica SP5–2photon confocal microscope using 100× oil objective with 3× digital zoom. Images were collected and analyzed with LASAF software, and final processing was performed using ImageJ64. To enable direct comparison, all images within a given experiment were taken under the same magnification and laser intensity settings. 10–15 cells were imaged for each sample per experiment, and data from at least two independent experiments were used for quantification of phenotypes. Colocalization was quantified using the JACoP plugin for ImageJ64, with 5–10 representative cells used from at least 2 independent experiments. Background corrections were specified manually in ImageJ64 before running JACoP analysis, with similar adjustments applied across all images per channel per experiment. For colocalization reported as % of channel A overlapping channel B (labeled A:B), overlap was quantified using Mander's coefficients calculated on the basis of automated threshold settings, with 0 and 1 corresponding to no colocalization and complete colocalization, respectively. For colocalization reported in the form of a coefficient (r), overlap was quantified using JACoP coefficients $k1$ and $k2$, where $r^2 = k1k2$.

Bimolecular Fluorescence Complementation (BiFC)—BiFC was used in combination with conventional IF microscopy (see above) to characterize complex formation between USP8 and atypical SH3 domain containing adaptor proteins in HeLa cells. Cells were seeded at $2.5–3 \times 10^5$ per well onto polylysine-coated glass coverslips (Corning) in 6-well tissue culture plates

and allowed to adhere overnight. Cells were co-transfected with 1.0 μg of VN-FLAG-USP8 or mutant and 0.5 μg of VC-HA-STAM1/STAM2/Grb2 with 0.25 μg of Myc-ubiquitin if applicable. Cells were incubated to allow adequate development of venus fluorescent protein (VFP) fluorescence (7.5–9 h), fixed in 4% paraformaldehyde, and immunostained as indicated (for detailed IF protocols see above).

Co-immunoprecipitation—For co-immunoprecipitation of USP8 with STAM1, HeLa cells co-transfected with USP8 or mutant and FLAG-STAM1 or mutant in 60-mm plates were lysed in 400 μl of co-immunoprecipitation buffer (20 mM Tris-HCl, pH 7.4, 150 mM NaCl, 5 mM EDTA, 1% Triton X-100, 5% glycerol, 10 mM NaF, 1 mM Na_3VO_4, protease inhibitor mixture, 1 mM PMSF) on ice, and lysates were clarified at 8000 rpm at 4 °C. FLAG-tagged material was immunoprecipitated with 3 μg of anti-FLAG antibody on ProteinG beads, rotating at 4 °C overnight. After incubation, samples were washed 5× in co-immunoprecipitation buffer, eluted with the addition of 2× SDS gel loading buffer containing 200 mM DTT, and analyzed by Western blot as indicated.

Peptide Synthesis and Fluorescence Polarization—High density peptide arrays were synthesized by semi-automated SPOT synthesis on an Intavis Multispot as previously described (40). USP8 peptides Fl-KNVPQVDRTKKPA, Fl-SGKVLSDRSTKPV, and Fl-TVTPMVNRENKPT were synthesized at the 0.25-mmol scale using Fmoc (*N*-(9-fluorenyl)-methoxycarbonyl) solid phase synthesis. Fluorescein-labeled probes were prepared through the reaction of C-terminal peptides with 5-(and-6)-carboxyfluorescein succinimidyl ester (Molecular Probes), purified by reverse-phase HPLC, and confirmed by mass spectrometry. The Slp-76 peptide (Fl-APSIDRSTKPA) was previously reported (19). Equilibrium dissociation constants (K_D) were determined by fluorescence polarization on a Beacon 2000 fluorescence polarization system (Invitrogen). Binding studies were conducted with 5 nM fluorescein-labeled peptides dissolved in PBS containing 100 μg/ml BSA and 1 mM DTT. Reaction mixtures were allowed to equilibrate for 10 min at room temperature before each measurement. All fluorescence polarization measurements were conducted at 22 °C. Data fitting and dissociation constant determination was carried out as previously described (19).

RESULTS

USP8 Depletion Accelerates EGFR Turnover through an Hrs-dependent Pathway—The role of USP8 in the regulation of EGFR ubiquitination and stability has been scrutinized in a number of recent studies. The current consensus in the literature indicates that USP8 functions to protect EGFR from ligand-induced down-regulation by virtue of direct deubiquitination of activated receptors (24, 27, 41). To address the mechanisms of USP8 action in this context, we examined the consequences of USP8 depletion on EGFR turnover in response to low concentrations (2.5 ng/ml) of stimulating ligand, EGF. Under these conditions, EGFR is expected to undergo canonical clathrin-mediated endocytosis with robust access to recycling as well as degradation (42). Consistent with previous reports, comparison of control cells and those transiently depleted of USP8 revealed an increase in the rate of EGFR turnover (Fig. 1, *A* and *B*; supplemental Fig. S1, *A* and *B*). Moreover, loss of USP8 resulted in increased ubiquitination of the receptor in the presence of EGF administered at the same concentration as above (Fig. 1*C*). Importantly, this effect on EGFR ubiquitination was observed early after stimulation (5 min) and, therefore, reflects changes taking place before intracellular sorting events.

EGFR is known to traffic through an endocytic pathway regulated by Hrs, and USP8 loss-of-function phenotypes are similar to those observed for Hrs. To examine whether USP8 and Hrs regulate EGFR through a common pathway, the effects of USP8 depletion on EGFR stability and degradation were assessed as a function of Hrs. As previously reported, knockdown of Hrs alone (*siHrs-1* (31) and *siHrs-2* (38)) disrupted receptor down-regulation compared with the control (Fig. 1*D*), whereas loss of USP8 accelerated receptor turnover in response to ligand treatment (Fig. 1, *D* and *E*). In addition, USP8 depletion resulted in marked destabilization of EGFR in the absence of acute stimulation with EGF (this phenotype became pronounced with a more severe loss of USP8 protein compared with a less stringent USP8 depletion, as in Fig. 1*A*, where decrease in EGFR levels at treatment time of 0 min was not readily observed). Both effects of USP8 depletion on EGFR stability were effectively counteracted by concomitant Hrs knockdown (Fig. 1, *D* and *E*). In fact, *siHrs-1*, which gave rise to only a partial loss of Hrs protein, afforded a lesser rescue of *siUSP8* compared with the more efficient *siHrs-2* (Fig. 1*D*), indicating that USP8 ablation induces a phenotype sensitive to the cellular concentration of Hrs. Collectively, these results demonstrate a critical role for USP8 in mitigating EGFR degradation via an Hrs-dependent pathway, suggesting a functional relationship between USP8 and Hrs in EGFR trafficking.

Central Region of USP8 Regulates EGFR Ubiquitination—USP8 is known to deubiquitinate EGFR in response to ligand stimulation; however, the molecular determinants required for this function have not been described. Similar to a previous report (27), inactivation of USP8 through either a point mutation in the catalytic cysteine residue (*C748A*) or a truncation of the entire catalytic domain (Δ*C*, Fig. 2*A*) resulted in acute hyperubiquitination of EGFR (Fig. 2, *B* and *C*), whereas overexpression of wild type enzyme led to diminished receptor ubiquitination (Ref. 27 and Fig. 2*C* (representative data are shown in Fig. 6*A*)). Overexpression of two N-terminal fragments of USP8 containing either the MIT domain alone (*MIT*) or in combination with the Rhodanese-like domain (*MIT-Rhod*) was insufficient to elicit a full-fledged USP8 loss-of-function phenotype (Fig. 2, *B* and *C*), indicating that the central region of the molecule is required for this function.

Because EGFR ubiquitination status dictates receptor trafficking, USP8 inactivation was expected to enhance localization of EGFR to ubiquitin-rich endosomes. Indeed, overexpression of USP8 catalytic mutant, Δ*C*, produced a 2.5-fold increase in co-localization of EGFR, internalized in response to ligand treatment, with HA-ubiquitin (Fig. 2, *D* and *E*). Similar results were also observed in cells expressing USP8-C748A (data not shown). As in the case of EGFR hyperubiquitination, enhanced receptor localization to ubiquitinated endosomes was abrogated upon deletion of the central region of USP8 (Fig. 2, *D* and

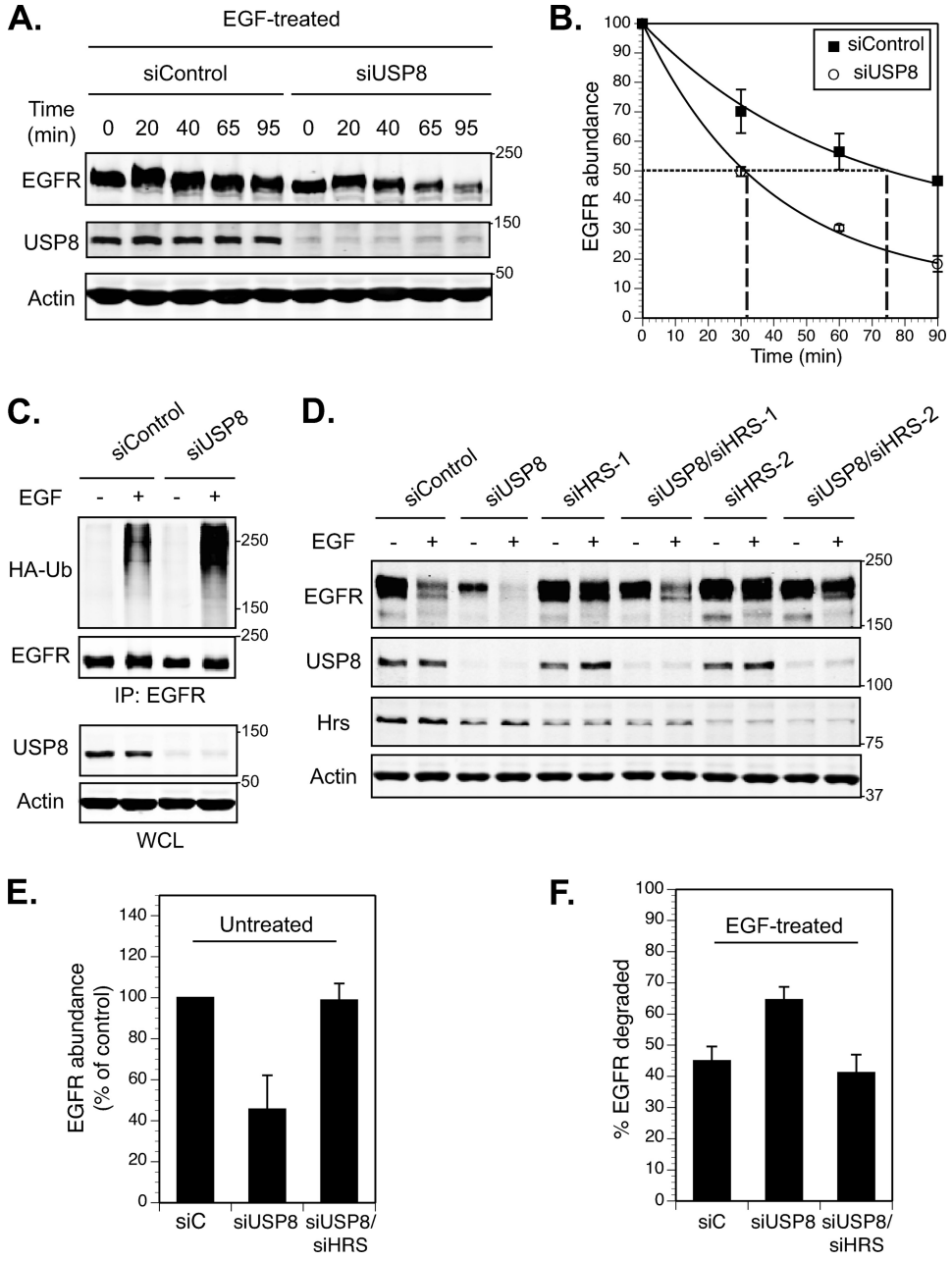

FIGURE 1. **USP8 depletion accelerates ligand-mediated EGFR degradation through an Hrs-dependent pathway.** *A* and *B*, USP8 knockdown induces accelerated EGFR turnover in response to EGF. HeLa cells transfected with either control siRNA (*siControl*) or siRNA targeting human USP8 (*siUSP8*) were serum-starved and treated in the presence of 2.5 ng/ml EGF for the specified length of time. Western blot analysis of total cellular EGFR observed throughout the treatment time course and efficiency of USP8 knockdown are shown. *B*, shown is a graphic representation of EGFR degradation rates as a function of USP8 (see "Materials and Methods" for details). *C*, USP8 depletion results in elevated ligand-induced ubiquitination of EGFR. Cells co-transfected with HA-ubiquitin (*HA-Ub*) and either siControl or siUSP8 were serum-starved and treated in the absence (−) or presence (+) of 2.5 ng/ml EGF for 5 min. EGFR was immunoprecipitated, and ubiquitination was analyzed by Western blot against HA. *D–F*, USP8 modulates EGFR degradation through an Hrs-dependent pathway. Cells transfected with siControl alone, co-transfected with siUSP8, siHrs, or a combination of the two were serum-starved and treated in the absence (−) or presence (+) of 2.5 ng/ml EGF for 1 h. *D*, shown is a Western blot analysis of endogenous proteins. Quantification of changes in EGFR abundance (relative to siControl) (*E*) and down-regulation (expressed as % of total EGFR in untreated cells (−)) (*F*) are shown. All quantification was performed on the basis of three independent experiments (n = 3), with *error bars* corresponding to S.D.

E). This region has been reported to contain STAM binding determinants (20, 21), and EGFR was found to traffic largely on STAM-positive endosomes during the timeframe consistent with USP8-dependent changes observed in both receptor ubiquitination and co-localization with endosomal ubiquitin (supplemental Fig. S2*A*). Moreover, overexpression of wild type STAM1/2 proteins produced a 50% increase in EGFR ubiquitination relative to vector control, whereas mutations in their respective SH3 domains abrogated the receptor phenotype (supplemental Fig. S2, *B* and *C*). These results indicate that the SH3 domains of STAM proteins modulate the ubiquitination status of EGFR, possibly through the recruitment of a critical deubiquitinating enzyme, such as USP8.

USP8 Contains Three Low Affinity RXXK Motifs That Facilitate the Interaction with Atypical SH3 Domains—We and others have previously reported a subfamily of SH3 domains that bind to atypical peptide ligands centered around a consensus R*XX*K peptide motif (19–21, 43–46). Belonging to this domain group are the C-terminal SH3 domains of the Grb2 family of adaptor proteins (Grb2, Gads, and Grap) as well as STAM1 and STAM2. Two consensus R*XX*K motifs had previously been identified in USP8 and shown to interact with the STAM2 SH3 domain (19–21). To identify any additional linear peptide epitopes in USP8 capable of supporting interactions with the R*XX*K-binding subfamily of SH3 domains in an unbiased manner, a SPOTs peptide array scan of the human USP8 protein sequence was probed with the C-terminal SH3 domain of adaptor protein Gads (GST-Gads-SH3C) (supplemental Fig. S3*A*). Gads SH3 was chosen on the basis of its documented high affinity for other known R*XX*K peptides (19, 43). As expected, binding of the GST-Gads-SH3C to peptides containing two previously identified R*XX*K motifs of USP8 was observed (supplemental Fig. S3*A*, *peptides 1*, *2*, *5*, and *6*). Two additional peptides (supplemental Fig. S3*A*, *peptides 3* and *4*) were found to interact with the SH3 domain of Gads. Peptide 4 (PVEGKRCPTSEA) was found to exhibit nonspecific binding to GST alone due to the presence of a highly reactive cysteine residue (data not shown). Peptide 3 (SDRSTKPVFPSP) was noted to contain a partial consensus

R*XXK* motif. The R*XXK* motif embedded in peptide 3 lacks the consensus N-terminal proline residue, the loss of which results in a partial loss of SH3 domain binding affinity (19) and is tolerated in the truncation of a previously described USP8 R*XXK* motif, corresponding to peptide 1. Mutation of the critical arginine to lysine abolished binding of GST-Gads-SH3C in each of the three R*XXK* peptides of USP8 (supplemental Fig. S3*A*, *peptides 7–12*), indicating that in each case the binding is depen-

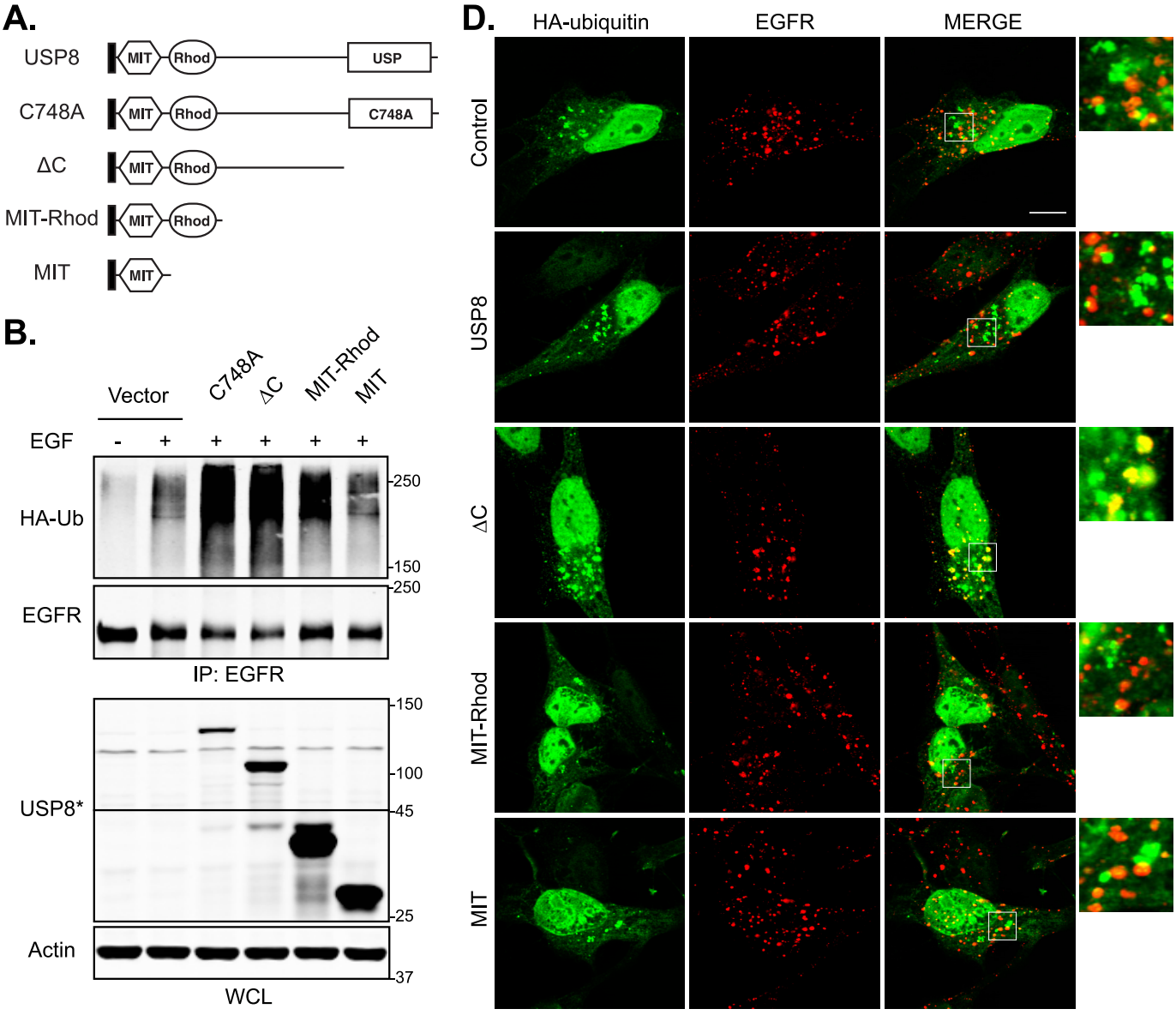

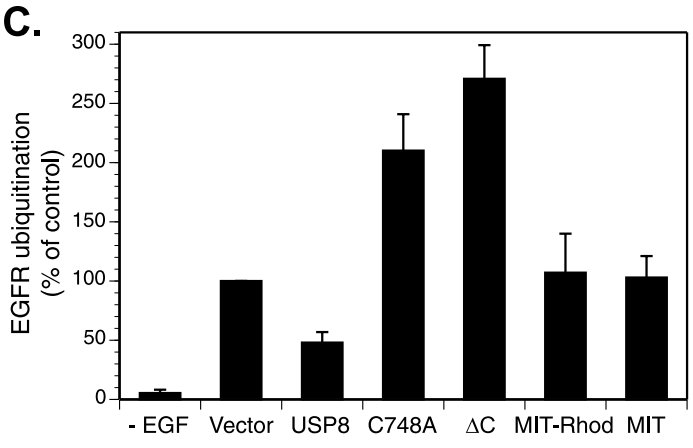

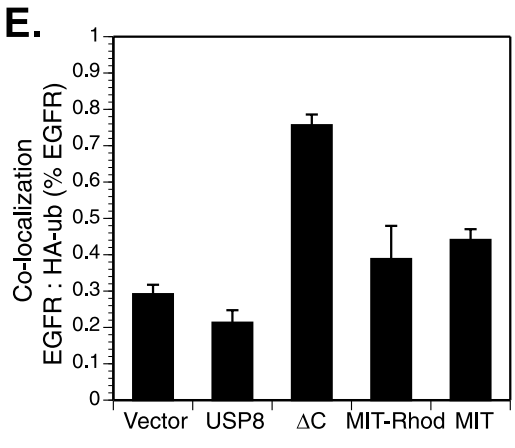

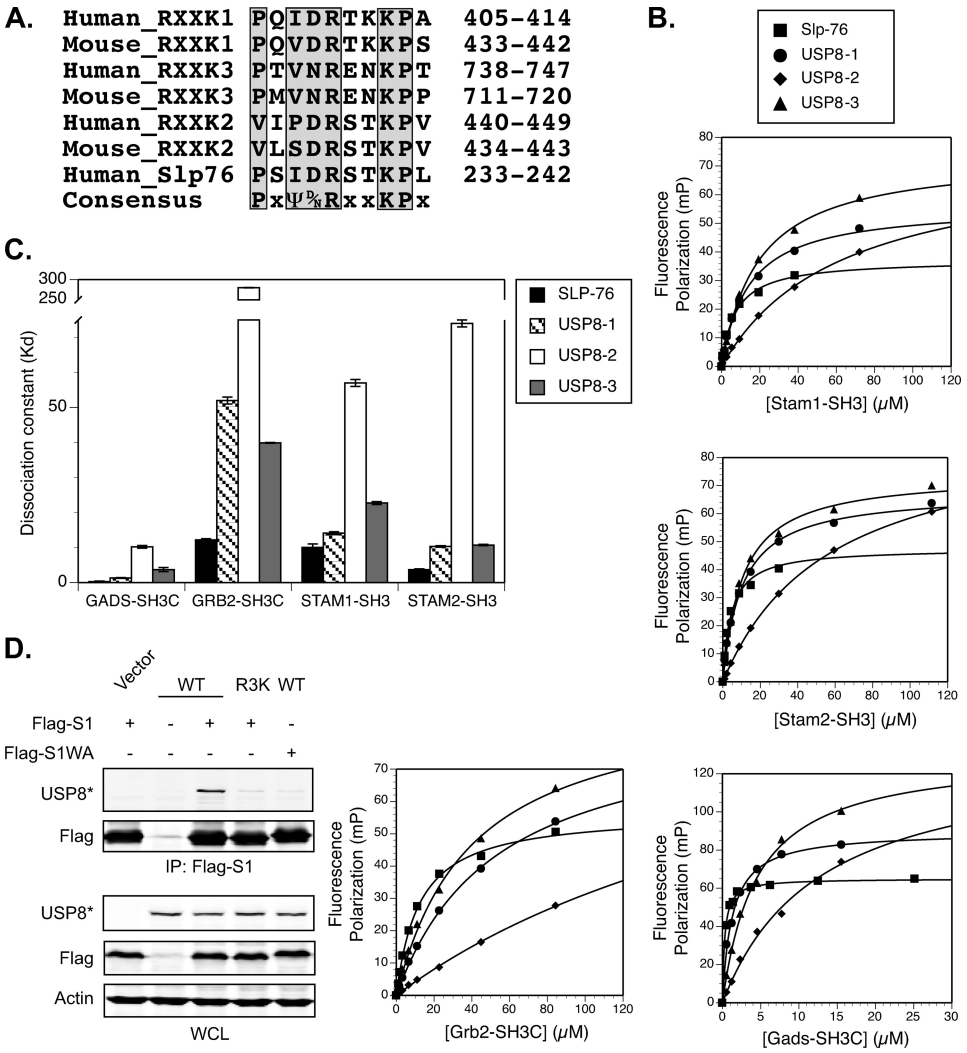

FIGURE 3. **USP8 contains three *RXXK* motifs that constitute low affinity binding partners for non-canonical SH3 domains.** *A*, ClustalW2 alignment of mouse and human USP8 protein sequences encompassing the three *RXXK* motifs of USP8 is shown. *B*, shown are SH3 domains of adaptor proteins exhibit low affinities for the *RXXK* peptides of USP8. Fluorescence polarization in millipolarization units (*mP*) was measured for fluorescein-tagged peptides corresponding to Slp76 (FI-APSIDRSTKPA) and USP8-1 (FI-KNVPQVDRTKKPA), USP8-2 (FI-SGKVLSDRSTKPV), and USP8-3 (FI-TVTPMVNRENKPT) as a function of GST-SH3 (measurements taken using Beakon 2000; data were plotted in DeltaGraph 5.7.5). *C*, shown is a graphic representation of equilibrium dissociation constants (K_D) obtained using fluorescence polarization (see "Materials and Methods"). The corresponding numerical values can be found in supplemental Fig. S3C. *D*, The USP8·STAM complex co-immunoprecipitates in a manner dependent upon the interaction between the *RXXK* motifs of USP8 and the SH3 domain of STAM. Lysates from cells co-transfected with wild type USP8 (*WT*) or the triple *RXXK* mutant (*R3K*) and *FLAG-STAM1* or its SH3 domain mutant, *FLAG-STAM1-WA*, were immunoprecipitated with anti-FLAG antibody, and samples were analyzed by Western blot against exogenous USP8 (*USP8**). All *error bars* correspond to S.D.

dent on this conserved motif. Arrayed next to each other (supplemental Fig. S3*A*, *peptides 7–9*), all three peptides from USP8 appear to support binding to the Gads SH3 domain.

To examine the ability of all three USP8 *RXXK* motifs to independently interact with adaptor SH3 domains in the context of their native USP8 protein sequence, co-precipitation experiments were performed using purified recombinant GST fusion proteins, corresponding to murine USP8 fragments Pro-393—Thr-428, Pro-432—Pro-630, and Pro-658—Pro-730 containing *RXXK*-1 (*R1*), *RXXK*-2 (*R2*), and *RXXK*-3 (*R3*), respectively. Lysates from cells transfected with either FLAG-tagged wild type Gads (FLAG-Gads) or a mutant in which the critical tryptophan of the C-terminal SH3 domain is mutated (FLAG-Gads-WA), rendering the SH3 domain incapable of binding *RXXK* peptides (19), were subjected to glutathione-precipitation with GST alone, GST-hSlp-76—Arg-204—Gly-395 (positive control), or individual GST-USP8 fragments (supplemental Fig. S3*B*). All three GST-*RXXK* fragments of USP8 were able to precipitate full-length Gads but not Gads-WA, confirming a requirement for a functional *RXXK* binding SH3 domain for the interaction of each of the three *RXXK* motifs within the USP8 primary sequence.

An alignment of the three *RXXK* motifs of USP8 from the mouse and human proteins indicates a high level of conservation (Fig. 3*A*). The second *RXXK* motif in USP8 (*R2*) lacks consensus residues N-terminal to Asp located at −1 relative to the conserved arginine in both species but maintains the core region corresponding to DR*XX*KP that contains the majority of the SH3 domain-contacting residues (43). To examine affinities of the USP8 *RXXK* peptides, the equilibrium dissociation constants were measured between

FIGURE 2. **The central region of USP8 is required to regulate EGFR ubiquitination.** *A*, domain organization and mutational analysis of USP8 is shown. Boundaries of individual domains and residues critical for domain function are indicated using amino acid numbering of murine USP8 (GenBank™ accession no. BC050947). *DUF*, Domain of Unknown Function 1873; *USP*, ubiquitin-specific protease domain with catalytic Cys 748. Truncation mutants of USP8 with amino acid boundaries are designated in *parentheses*: Δ*C*, catalytic domain truncation (amino acid residues 1–735); *MIT* (amino acid residues 1–184); *MIT-Rhod* (amino acid residues 1–319). All USP8 mutants were constructed on the basis of available structural data (20, 33). *B*, catalytic inactivation of USP8 leads to EGFR hyperubiquitination in a manner dependent upon the central region of the enzyme. Cells co-transfected with HA-ubiquitin and vector control or USP8 mutants as indicated were serum-starved and treated in the absence (−) or presence (+) of 10 ng/ml EGF for 10 min. EGFR ubiquitination was assayed as in Fig. 1*C* and quantified relative to EGF-treated vector control samples; $n = 3$ (*C*). *D*, catalytically inactive USP8 results in enhanced localization of EGFR to intracellular ubiquitin and requires the central region of USP8. Cells were transfected as indicated, serum-starved, and treated with EGF as above. After treatment, cells were fixed and immunostained against HA-ubiquitin (*green*) and EGFR (*red*). Representative images are shown with 9× inset magnification; the *scale bar* corresponds to 10 μm. *E*, localization of EGFR to HA-ubiquitin was calculated as described under "Materials and Methods" and is represented as a fraction of EGFR overlapping HA-ubiquitin relative to total cellular EGFR; $n = 2$. All *error bars* correspond to S.D.

synthetic peptides corresponding to each R*XX*K motif and the SH3 domains of Gads, Grb2, STAM1, and STAM2 by fluorescence polarization (Fig. 3, *B* and *C*, and supplemental Fig. S3*C*). Individually, each of the three R*XX*K motifs of USP8 was found to exhibit lower affinities for the R*XX*K subclass of SH3 domains than any of the previously measured interactions with single R*XX*K motifs in Slp76, Blnk, Gab1, or Gab2 (19). USP8 motifs R1 and R3 exhibit greater affinity for each SH3 domain than does R2, although peptides corresponding to each of the three sites bound with measurable affinity, suggesting that each one may contribute to binding in the context of the USP8 protein. The mutation of all three R*XX*K motifs in USP8 or a single mutation in the SH3 domain of STAM1 abrogated binding between the full-length proteins (Fig. 3*D*), underscoring the requirement for the R*XX*K/SH3 interaction to support direct complex formation.

Although the complex between the R*XX*K motifs of USP8 and the SH3 domains of STAM has previously been speculated to promote USP8 function on endosomes, no experimental evidence to that end has been produced. To characterize the R*XX*K-mediated complex formation in cells, BiFC microscopy was employed. BiFC takes advantage of a GFP variant, VFP, separated into N- and C-terminal fragments (VN and VC, respectively) that are fused to epitope-tagged proteins of interest. When co-expressed in cells, upon direct contact the VN- and VC- fused proteins form an irreversible fluorescent VFP complex visualized by standard microscopic techniques (Fig. 4*A*). In the USP8 assay, USP8 was fused to the VN fragment (VN-FLAG-USP8), and SH3 domain-containing adaptor proteins were incorporated into the VC construct (VC-HA-STAM2, -STAM1, or -Grb2, Fig. 4*B*). Cells co-transfected with wild type USP8 and STAM1 showed punctate fluorescence that immunostained positive for both FLAG and HA tags, confirming localization of individual proteins to the VFP signal (Fig. 4*C*, *panel 1*). BiFC of the USP8·STAM1 complex exhibited dependence on the SH3 domain of STAM1, as illustrated by the lack of bright VFP puncta in cells expressing the mutant *VC-STAM1-WA* (Fig. 4*C*, *panel 2*). Consistent with significantly lower affinity of the Grb2 SH3 domain for the USP8 R*XX*K peptides (Fig. 3, *B* and *C*), no VFP-positive complex appeared to form between USP8 and Grb2 on the incubation time scale sufficient to observe the USP8·STAM1 BiFC (Fig. 4*C*, *panel 3*), suggesting that Grb2 does not constitute a primary binding partner for USP8.

As in the case of STAM1, USP8·STAM2 BiFC produced robust VFP-positive puncta that were not observed with the triple R*XX*K mutant of USP8 (Fig. 4*C*, *panels 4* and *5*), confirming that the complex forms in a manner requiring the R*XX*K/SH3 interaction. Furthermore, the ability of the catalytic domain truncation mutant of USP8, VN-FLAG-ΔC, to readily participate in the BiFC complex with STAM2 (Fig. 4*C*, *panel 6*) indicated that VFP fluorescence is not observed due to a nonspecific interaction between the ubiquitin-specific peptidase (USP) domain of USP8 and ubiquitinated STAM on endosomes.

USP8·STAM Complex Localizes to the ESCRT-0 and Modulates Ubiquitin Dynamics on EGFR-positive Endosomes—To characterize the subcellular localization of the USP8·STAM complex, we examined overlap of its BiFC with relevant endosomal markers. Consistent with previously established localization and function of these proteins individually at the early-to-intermediate endosome, the USP8·STAM2 VFP extensively colocalized with endogenous ESCRT-0 components, STAM1 and Hrs (Fig. 5, *A*, *B*, and *D*) but did not exhibit appreciable colocalization with a late MVB marker, CD63 (Fig. 5, *C* and *D*). As localization of overexpressed proteins does not necessitate functional relevance, we assessed the contribution of the R*XX*K

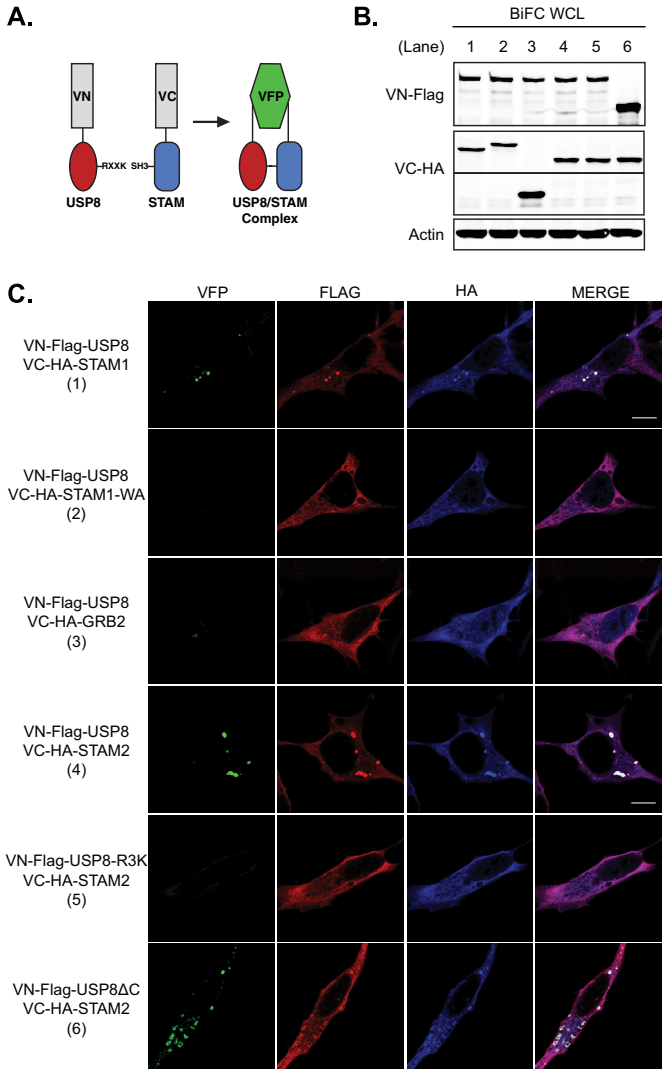

FIGURE 4. **Complex formation between USP8 and the SH3 domains of STAM proteins in their cellular context requires the R*XX*K/SH3 interaction.** *A*, shown is a schematic representation of the BiFC assay. In this assay USP8 was fused to the N-terminal and SH3-containing adaptor proteins to the C-terminal fragments of VFP. VFP fluorescence was observed upon direct interaction between individually non-fluorescent VN and VC fusion proteins co-expressed in live cells. *B*, shown is BiFC fusion protein expression as analyzed by Western blot against *VN-FLAG* and *VC-HA*. *C*, complex formation between USP8 and STAM1/2 proteins requires the SH3 domain of STAM as well as the R*XX*K motifs of USP8 but not its catalytic domain (numbering of samples corresponds to the order of lanes in *B*). Cells were transfected with VN-FLAG-USP8 or its triple R*XX*K mutant, *−R3K*, in combination with either VC-VN-HA-STAM1, SH3 domain mutant -STAM1-WA (as shown in Fig. 3D, this mutant fails to interact with USP8), -GRB2, or -STAM2. After incubation adequate for visualization of BiFC complexes by VFP fluorescence (*green*), cells were fixed and immunostained against FLAG (*red*) and HA (*blue*). All images were taken under the same magnification, with the *scale bar* corresponding to 10 μm.

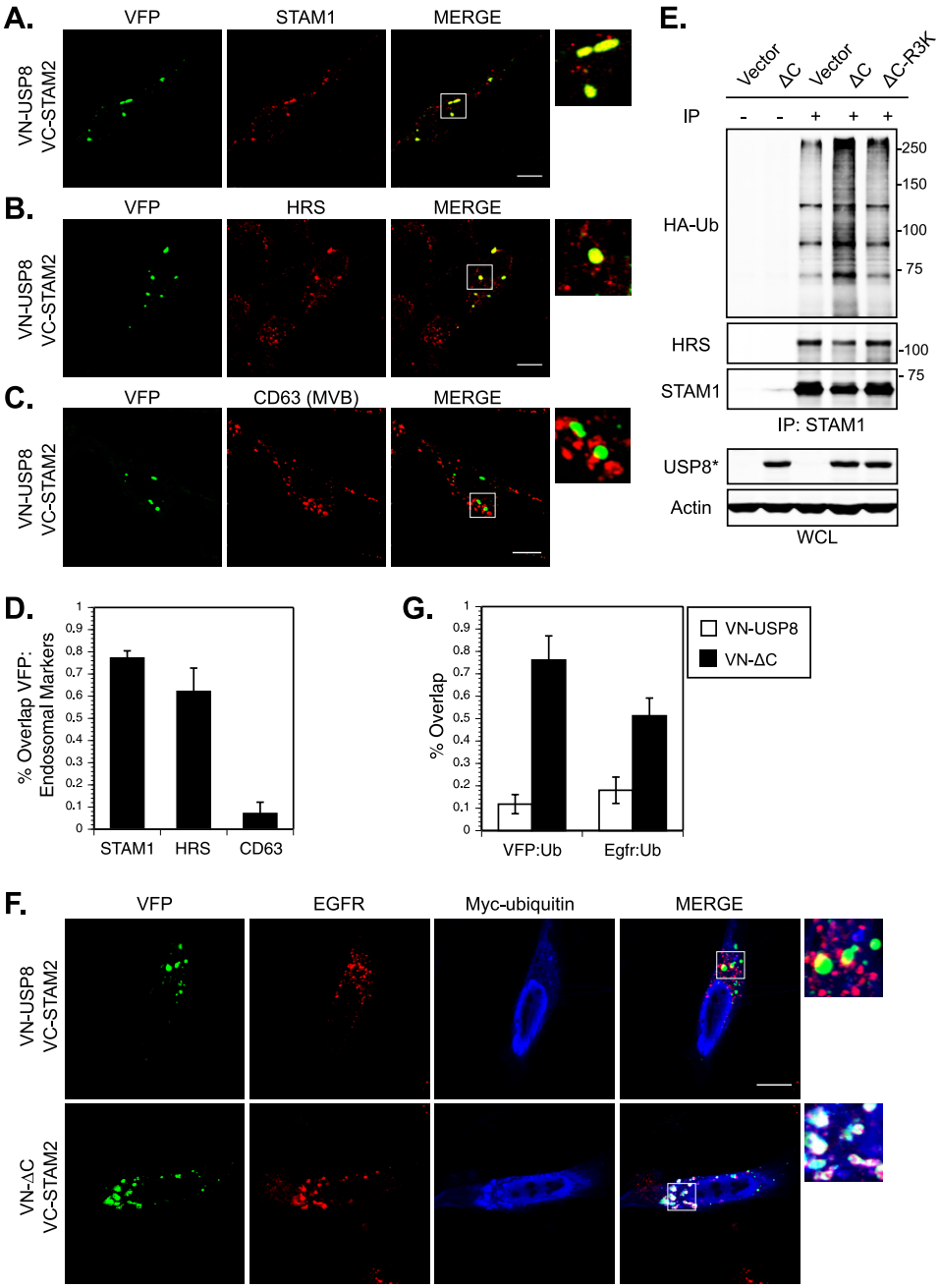

FIGURE 5. **The USP8·STAM complex localizes to the ESCRT-0-complex and regulates ubiquitin dynamics on EGFR-positive endosomes.** *A–D*, the USP8·STAM BiFC complex localizes to endosomes populated by the endogenous ESCRT-0 proteins, STAM1 (*A*) and Hrs (*B*), but not a late MVB marker, CD63 (*C*). Cells were co-transfected with VN-FLAG-USP8 and VC-HA-STAM2, fixed, and immunostained as indicated. *D*, quantification of colocalization between USP8·STAM BiFC and STAM1, Hrs, or CD63 is represented as a fraction of VFP fluorescence overlapping the indicated endosomal proteins; $n = 3$. *E*, overexpression of a catalytically inactive USP8 results in hyperubiquitination of the endogenous STAM·Hrs complex in a manner dependent upon the R*XX*K motifs. Cells were co-transfected with HA-ubiquitin (*HA-Ub*) and vector control or catalytically inactive USP8 containing either intact (Δ*C*) or mutated (Δ*C-R3K*) R*XX*K motifs. Endogenous ESCRT-0 complex was immunoprecipitated against the STAM1 protein as indicated, and its ubiquitination status was assessed by Western blot against HA. *F*, the USP8·STAM complex regulates ubiquitin dynamics on EGFR-positive endosomes. Cells expressing either *V*N-USP8 or VN-ΔC in combination with VC-STAM2 and Myc-ubiquitin were incubated under standard growth conditions to allow development of VFP fluorescence (*green*), briefly serum-starved, and treated in the presence of 10 ng/ml EGF for 30 min. After treatment, cells were fixed and immunostained against EGFR (*red*) and Myc (*blue*). Similar results were obtained with an EGF stimulation of 10 min (data not shown). All images are shown with 9× *inset* magnification and *scale bars* corresponding to 10 μm. *G*, co-localization of USP8·STAM BiFC and EGFR with Myc-ubiquitin is enhanced upon catalytic inactivation of USP8. Quantification of data is shown in *F*; $n = 2$. All *error bars* correspond to S.D.

motifs to the regulation of ESCRT-0 ubiquitination status by USP8. Hyperubiquitination of the STAM1·Hrs complex was observed in the presence of catalytically inactive Δ*C* compared with vector control (Fig. 5*E*) and wild type USP8 (supplemental Fig. S4*A*). Strikingly, the ubiquitination status of these proteins was largely unaffected in cells expressing the inactive triple R*XX*K mutant of USP8, Δ*C-R3K* (Fig. 5*E*). By contrast to STAM1, ubiquitination of Grb2 was not affected by USP8 loss-of-function (supplemental Fig. S4*B*). Thus, consistent with the BiFC data, these results functionally substantiate the notion that the R*XX*K motifs specify interaction(s) critical for USP8 function associated with ESCRT-0.

Results presented in Fig. 2 suggest a role for the USP8·STAM complex in trafficking of EGFR into ubiquitin-rich endosomal sub-compartments. Using USP8·STAM2 BiFC, colocalization of EGFR with ubiquitin was assessed as a function of USP8 catalytic activity. In cells expressing wild type USP8, neither the VFP-positive complexes nor EGFR, internalized in the presence of EGF, appreciably overlapped with Myc-ubiquitin (Fig. 5, *F* and *G*). Conversely, the catalytically inactive ΔC/STAM2 VFP exhibited broad colocalization with ubiquitin-positive endosomes populated by EGFR (Fig. 5, *F* and *G*), supporting a role for the interaction between USP8 and STAM in EGFR trafficking.

The RXXK Motifs Are Critical for Deubiquitination and Trafficking of EGFR by USP8—The ubiquitination studies described in Fig. 2 and supplemental Fig. S2 imply that USP8 may deubiquitinate activated EGFR when in complex with STAM. To address this hypothesis, we examined the contribution of the R*XX*K motifs to the overexpression phenotype of USP8. The ability of USP8 to reduce EGFR ubiquitination in response to stimulation with EGF (Fig. 6, *A–C*) was severely compromised by mutations in the three R*XX*K motifs (*R3K*). By contrast,

deletion of the MIT domain (Δ*MIT*) did not impinge on USP8 activity in this regard (Fig. 6, *A–C*). These results demonstrate that USP8 employs R*XX*K-mediated interaction(s), but not those afforded by the MIT domain, to influence ligand-induced ubiquitination of EGFR. Because receptor ubiquitination status dictates its endocytic sorting, the above observations

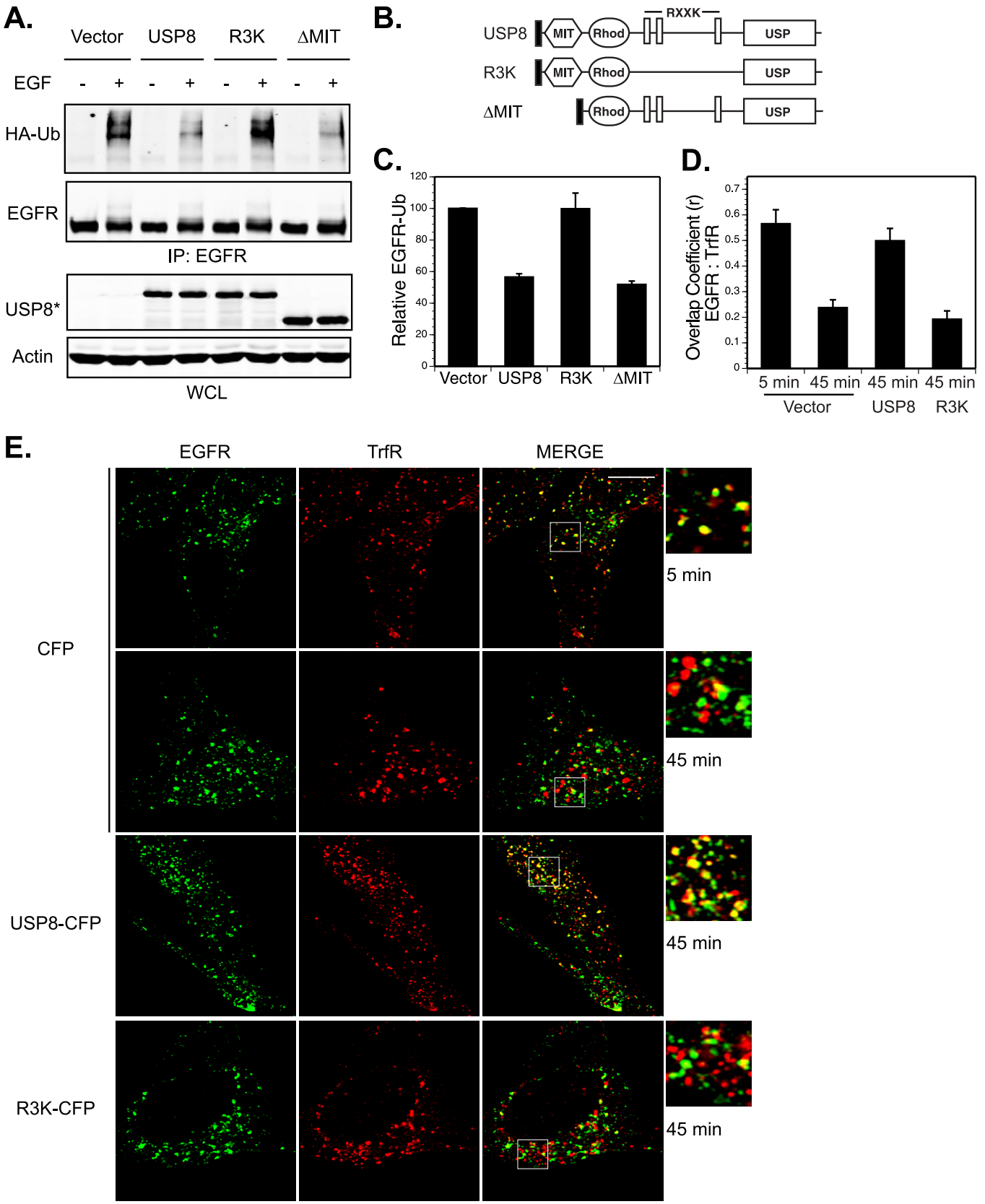

imply that the R*XX*K mutant of USP8 should also be deficient in protecting EGFR against trafficking downstream of the ubiquitination event. Specifically, in cells expressing *CFP* alone, treatment with EGF initially (5 min) induced broad co-localization of EGFR with constitutively internalized and recycled transferrin receptor (*TrfR*) (Fig. 6, *D* and *E*). However, at 45 min after stimulation, overlap between EGFR and TrfR fell by more than 50%, corresponding to progression of EGFR beyond TrfR-positive endosomes (Fig. 6, *D* and *E*). By contrast, cells overexpressing wild type *USP8-CFP* maintained a high degree of EGFR to TrfR overlap at 45 min post-treatment with EGF, whereas the R*XX*K mutations (R3K-CFP) abrogated this phenotype, with EGFR exhibiting a localization profile similar to that of the control (Fig. 6, *D* and *E*). Expression of USP8 was not found to significantly alter the extent of EGFR localization to TrfR-positive endosomes at the time point after receptor stimulation, implying that the delay in receptor trafficking did not occur before its encounter with the sorting endosome (data not shown). As EGFR stabilization against lysosomal turnover requires deubiquitination by USP8 (Figs. 1 and 6*A*) but TrfR is not subject to USP8-medited regulation (supplemental Fig. S1*A*), these findings reveal a critical role for the R*XX*K motifs in controlling EGFR trafficking beyond the early-to-recycling endosome circuit.

DISCUSSION

Reversible ubiquitination signals trafficking of endocytosed cell-surface receptors (47) and thereby influences receptor fate. Although research in this area has largely focused on the E3 enzymes, our understanding of the equally important DUBs remains rather rudimentary. This is particularly evident in the case of EGFR endocytosis, where the Cbl-family ubiquitin ligases are known to account for the total cellular ubiquitination of EGFR, and their respective localization to activated receptor complexes at specific trafficking stages have been described (7). By contrast, despite the insights gleamed from recent studies (24, 27, 32), the role of deubiquitination at these critical waypoints in EGFR trafficking remains unclear.

Deciphering the complexity of DUB biology in receptor endocytosis necessitates an understanding of protein-protein interactions that inform enzyme recruitment to various endosomal subcompartments and substrates contained therein. Two ESCRT-associated DUBs, USP8 and AMSH, have been implicated in the EGFR pathway with opposing consequences for ligand-mediated receptor turnover. Unlike AMSH, which does not directly regulate EGFR (27) but functions to generally promote cargo trafficking through the sorting endosome (48), USP8 is required to deubiquitinate and, thus, protect EGFR from lysosomal degradation (24, 27, 41). Although the association of USP8 with the ESCRT machinery has been previously speculated to target the DUB to its EGFR substrate on endosomes, the ability of USP8 to influence receptor ubiquitination and turnover by virtue of such interaction(s) has not been described. To address the mechanisms underlying USP8 function in this context, the present study has characterized USP8 recruitment to the ESCRT-0 complex via the SH3 domain(s) of STAM proteins and evaluated its implications for the deubiquitination and trafficking of EGFR.

In agreement with published evidence, our loss-of-function studies indicate a requirement for USP8 in EGFR stabilization (24, 27, 41) and demonstrate that accelerated receptor degradation, resulting from USP8 depletion, proceeds through a pathway controlled by Hrs (Fig. 1). Consistent with these findings, ectopic expression of a catalytically inactive USP8 leads to enhanced EGFR ubiquitination, which occurs in a manner dependent upon the central region of USP8, harboring STAM binding determinants (Fig. 2). Moreover, overexpression of a "dominant negative" USP8 catalytic domain truncation mutant elicits enhanced colocalization of internalized EGFR with ubiquitin-rich endosomes, whereas the N-terminal MIT and Rhod domains appear insufficient to produce this phenotype (Fig. 2). The above effects of USP8 inactivation are observed nearly immediately after stimulation with EGF (5–10 min), a time when a substantial portion of the receptor travels on STAM-positive endosomes (supplemental Fig. S2). Not surprisingly, overexpression of STAM proteins under these conditions results in elevated levels of EGFR ubiquitination, presumably due to titration of cognate DUB activity away from the receptor substrate (supplemental Fig. S2). As mutations in the SH3 domains of STAM1/2 abrogate the overexpression effect, these results imply a role for the SH3 domains in recruitment of a critical DUB to the ubiquitinated EGFR.

Ubiquitin-dependent trafficking of endocytosed EGFR proceeds in at least two phases, with each characterized by a discrete ubiquitination event (7). During the early phase c-Cbl ubiquitinates EGFR at the plasma membrane immediately after activation by EGF to signal the initial receptor selection for the MVB. Subsequently, Cbl-b ubiquitinates EGFR in the second phase, required for the irrevocable commitment to degradation. Although it has been appreciated for some time that USP8 promotes EGFR deubiquitination, previous studies have not addressed the temporal aspects of USP8 function in this context. Our work demonstrates that hyperubiquitination of EGFR in cells compromised for USP8 activity occurs quickly (5–10 min) after stimulation on a timescale adequate for receptor internalization and possibly progression to the sorting endosome but not sufficient to allow late trafficking events to take place (Ref. 49, Fig. 6, and data not shown). The two phases of EGFR ubiquitination are presumably coupled to the early or

FIGURE 6. **The USP8·STAM complex regulates EGFR ubiquitination and trafficking.** *A*, the R*XX*K motifs are essential for USP8-mediated deubiquitination of EGFR, whereas the MIT domain does not contribute to this function. Cells co-transfected with HA-ubiquitin (*HA-Ub*) and vector, USP8, R3K, or ΔMIT (constructs shown in *B*) were serum-starved and treated in the absence (−) or presence (+) of 10 ng/ml EGF for 10 min. EGFR ubiquitination was analyzed as in Fig. 2*B*. *C*, shown is quantification of the data in *A*; $n = 3$. *D*, USP8 requires the R*XX*K motifs to modulate transit of EGFR through the transferrin receptor (*TrfR*)-positive endosomes. Cells, transfected with *CFP*, *USP8-CFP*, or *R3K-CFP* were serum-starved, treated with 10 ng/ml EGF for 5 or 45 min, as indicated, fixed, and immunostained against TrfR (*green*) and EGFR (*red*). CFP-positive cells are shown (CFP fluorescence not provided) with 9× *inset* magnification and *scale bars* corresponding to 10 μm. *E*, colocalization between EGFR and TrfR is expressed in the form of an overlap coefficient, *r* (see "Materials and Methods" for details); $n = 2$. All *error bars* correspond to S.D.

late sorting complexes, respectively, which are required to decipher the ubiquitination signals and execute appropriate trafficking tasks. As Hrs and STAM comprise the ESCRT-0 complex implicated in the early steps of receptor trafficking (18, 50), our observations, therefore, imply that STAM-mediated recruitment of USP8 for deubiquitination at this juncture may curtail EGFR sorting into the late endosomal compartments.

Although both EGFR and STAM have formerly been identified as USP8 substrates, the molecular determinants responsible for targeting USP8 activity to these proteins in their cellular context have not been elucidated. We and others have previously reported two motifs in USP8 that interact with atypical SH3 domains of proteins belonging to the Grb2 and STAM adaptor families (19, 45, 51). Although the classical SH3 domains bind to proline-rich ligands that assume a polyproline type II helix (52), this subfamily of SH3 domains interacts with R-*XX*K ligands, which take on a characteristic 3_{10} helical conformation (43). To assess whether USP8 contains additional motifs capable of interacting with SH3 domains, we exhaustively tested USP8 sequence determinants against a high affinity SH3 domain of Gads (Fig. 3, supplemental Fig. S3). In the course of these studies, we identified a novel partial consensus R*XX*K site in USP8 and determined that all three USP8 motifs constitute low affinity SH3 binding partners, with equilibrium dissociation constants in the μM to 10s of μM range (Fig. 3). The biochemical characterization of these interactions is consistent with transient association between USP8 and relevant proteins *in vivo*, well suited to support recruitment of USP8 to a dynamic cellular compartment, such as the endocytic pathway.

If the R*XX*K motifs of USP8 are necessary and sufficient to specify a direct interaction with SH3 domains *in vitro*, do they similarly inform USP8 localization and function in the cell? Due to the broad cellular distribution of USP8 (25, 27, 32, 34, 35), ascribing loss of a specific protein-protein interaction has previously proven elusive. Earlier attempts employing conventional fluorescence microscopy revealed no discernable contribution from the regions containing these motifs to the enzyme endosomal localization profile (27). Similarly, no phenotypic outcomes for disrupting the USP8·STAM interaction in endocytosis have been identified. Nevertheless, strict conservation of all three R*XX*K motifs between mouse and human USP8 proteins (Fig. 3) implies functional relevance for their interactions *in vivo*. The present study applied a 2-fold approach to examining the role of R*XX*K-mediated USP8 recruitment in the regulation of ubiquitination and trafficking of EGFR. First, BiFC microscopy was employed (39) to distinguish mere colocalization of USP8 and STAM on endosomes from the formation of a *bona fide* USP8·STAM complex. Second, the effects of disrupting the R*XX*K motifs on deubiquitination of relevant USP8 substrates were assessed. Using split VFP fluorophore protein fusions, we found the fluorescent BiFC complex to be readily reconstituted in an R*XX*K- and SH3 domain-dependent manner between USP8 and either STAM1 or STAM2, whereas BiFC between USP8 and Grb2 was not observed (Fig. 4). Consistent with these observations, R*XX*K-mediated localization of USP8 to ESCRT-0-positive endosomes was found to modulate the ubiquitination status of the Hrs/STAM complex (Figs. 4 and 5). Conversely, ubiquitination of Grb2 was not affected by USP8, revealing specificity of USP8 toward the SH3 domains of STAM proteins.

Although it has previously been speculated that STAM-mediated recruitment of USP8 to the sorting endosome may constitute an important regulatory mechanism in EGFR trafficking (21, 29), no direct experimental evidence in support of this model has been produced (27). As visualized with BiFC, EGFR internalized in response to EGF stimulation encounters the USP8·STAM complex and, in the presence of a catalytically inactive USP8, overlaps with subcellular regions of high ubiquitin content (Fig. 5). These observations illustrate a functional relationship between the deubiquitinating activity of USP8 and ligand-mediated trafficking of EGFR through the ESCRT-0 checkpoint. Collectively, USP8 loss-of-function studies presented herein imply that forming a complex with STAM is required for effective receptor deubiquitination by USP8. Indeed, overexpression experiments demonstrate EGFR deubiquitination to be fully contingent upon the three R*XX*K motifs of USP8 (Fig. 6). By contrast, deletion of the MIT domain does not impinge upon the efficacy of USP8 function in this respect. As the MIT domain reportedly interacts with the ESCRT-III proteins (32), it likely constitutes a late endosomal localization determinant irrelevant to the early phase of EGFR trafficking directly controlled by USP8.

Because EGFR ubiquitination status dictates partitioning of endocytosed receptors between recycling and degradation, these findings, therefore, implicate the R*XX*K motifs in receptor trafficking downstream of the targeting ubiquitination event. Specifically, if deubiquitination protects against Hrs-dependent trafficking of EGFR for proteolysis, increase in the cellular concentration of USP8 should prevent (or delay) receptor sorting away from the early-to-recycling endosome pathway. This model is supported by the observations demonstrating that USP8 overexpression attenuates progression of EGFR away from transferrin receptor-positive endosomes, whereas disruption of the USP8·STAM complex through mutations in the R*XX*K motifs is sufficient to abrogate the trafficking delay (Fig. 6). Taken together, these findings demonstrate that USP8 and the ESCRT-0 machinery constitute a key regulatory mechanism for the determination of EGFR fate after endocytosis and in doing so link reversible ubiquitination to the spatiotemporal regulation of receptor trafficking.

Acknowledgments—We thank Marsha Rosner (University of Chicago), Lawrence Dick (Millennium/Takeda), and Brett Engelmann (University of Chicago) for critical reading of the manuscript. We also thank Vytas Bindokas for invaluable advice regarding confocal imaging and Maria Sierra, Kate Higginbotham, Michelle Wright, Rebecca Dise, Bernard Liu, and Eshana Shaw for reagents and helpful discussion. BiFC expression vectors pBiFC-VN173-FLAG and pBiFC-VC155-HA were kindly provided by Chang-Deng Hu (Purdue University), and ubiquitin cDNA was a gift from Susan Conzan.

REFERENCES

1. Polo, S., and Di Fiore, P. P. (2006) *Cell* **124,** 897–900
2. Pickart, C. M. (2001) *Annu. Rev. Biochem.* **70,** 503–533
3. Haglund, K., Sigismund, S., Polo, S., Szymkiewicz, I., Di Fiore, P. P., and

Dikic, I. (2003) *Nat. Cell Biol.* **5,** 461–466
4. Hicke, L., and Riezman, H. (1996) *Cell* **84,** 277–287
5. Duan, L., Miura, Y., Dimri, M., Majumder, B., Dodge, I. L., Reddi, A. L., Ghosh, A., Fernandes, N., Zhou, P., Mullane-Robinson, K., Rao, N., Donoghue, S., Rogers, R. A., Bowtell, D., Naramura, M., Gu, H., Band, V., and Band, H. (2003) *J. Biol. Chem.* **278,** 28950–28960
6. Huang, F., Kirkpatrick, D., Jiang, X., Gygi, S., and Sorkin, A. (2006) *Mol. Cell* **21,** 737–748
7. Pennock, S., and Wang, Z. (2008) *Mol. Cell. Biol.* **28,** 3020–3037
8. Raiborg, C., and Stenmark, H. (2009) *Nature* **458,** 445–452
9. Shih, S. C., Katzmann, D. J., Schnell, J. D., Sutanto, M., Emr, S. D., and Hicke, L. (2002) *Nat. Cell Biol.* **4,** 389–393
10. Hanyaloglu, A. C., McCullagh, E., and von Zastrow, M. (2005) *EMBO J.* **24,** 2265–2283
11. Kanazawa, C., Morita, E., Yamada, M., Ishii, N., Miura, S., Asao, H., Yoshimori, T., and Sugamura, K. (2003) *Biochem. Biophys. Res. Commun.* **309,** 848–856
12. Raiborg, C., Bache, K. G., Gillooly, D. J., Madshus, I. H., Stang, E., and Stenmark, H. (2002) *Nat. Cell Biol.* **4,** 394–398
13. Urbé, S., Sachse, M., Row, P. E., Preisinger, C., Barr, F. A., Strous, G., Klumperman, J., and Clague, M. J. (2003) *J. Cell Sci.* **116,** 4169–4179
14. Shields, S. B., Oestreich, A. J., Winistorfer, S., Nguyen, D., Payne, J. A., Katzmann, D. J., and Piper, R. (2009) *J. Cell Biol.* **185,** 213–224
15. Haglund, K., Di Fiore, P. P., and Dikic, I. (2003) *Trends Biochem. Sci* **28,** 598–603
16. Hoeller, D., Crosetto, N., Blagoev, B., Raiborg, C., Tikkanen, R., Wagner, S., Kowanetz, K., Breitling, R., Mann, M., Stenmark, H., and Dikic, I. (2006) *Nat. Cell Biol.* **8,** 163–169
17. Ren, J., Kee, Y., Huibregtse, J. M., and Piper, R. C. (2007) *Mol. Biol. Cell* **18,** 324–335
18. Ren, X., Kloer, D. P., Kim, Y. C., Ghirlando, R., Saidi, L. F., Hummer, G., and Hurley, J. H. (2009) *Structure* **17,** 406–416
19. Berry, D. M., Nash, P., Liu, S. K., Pawson, T., and McGlade, C. J. (2002) *Curr. Biol.* **12,** 1336–1341
20. Kaneko, T., Kumasaka, T., Ganbe, T., Sato, T., Miyazawa, K., Kitamura, N., and Tanaka, N. (2003) *J. Biol. Chem.* **278,** 48162–48168
21. Kato, M., Miyazawa, K., and Kitamura, N. (2000) *J. Biol. Chem.* **275,** 37481–37487
22. Kim, M. S., Kim, J. A., Song, H. K., and Jeon, H. (2006) *Biochem. Biophys. Res. Commun.* **351,** 612–618
23. Naviglio, S., Mattecucci, C., Matoskova, B., Nagase, T., Nomura, N., Di Fiore, P. P., and Draetta, G. F. (1998) *EMBO J.* **17,** 3241–3250
24. Niendorf, S., Oksche, A., Kisser, A., Löhler, J., Prinz, M., Schorle, H., Feller, S., Lewitzky, M., Horak, I., and Knobeloch, K. P. (2007) *Mol. Cell. Biol.* **27,** 5029–5039
25. Mizuno, E., Kobayashi, K., Yamamoto, A., Kitamura, N., and Komada, M. (2006) *Traffic* **7,** 1017–1031
26. Alwan, H. A., and van Leeuwen, J. E. (2007) *J. Biol. Chem.* **282,** 1658–1669
27. Mizuno, E., Iura, T., Mukai, A., Yoshimori, T., Kitamura, N., and Komada, M. (2005) *Mol. Biol. Cell* **16,** 5163–5174
28. Mizuno, E., Kitamura, N., and Komada, M. (2007) *Exp. Cell Res.* **313,** 3624–3634
29. Row, P. E., Prior, I. A., McCullough, J., Clague, M. J., and Urbé, S. (2006) *J. Biol. Chem.* **281,** 12618–12624
30. Komada, M., and Kitamura, N. (2005) *J. Biochem.* **137,** 1–8
31. Lu, Q., Hope, L. W., Brasch, M., Reinhard, C., and Cohen, S. N. (2003) *Proc. Natl. Acad. Sci. U.S.A.* **100,** 7626–7631
32. Row, P. E., Liu, H., Hayes, S., Welchman, R., Charalabous, P., Hofmann, K., Clague, M. J., Sanderson, C. M., and Urbé, S. (2007) *J. Biol. Chem.* **282,** 30929–30937
33. Avvakumov, G. V., Walker, J. R., Xue, S., Finerty, P. J., Jr., Mackenzie, F., Newman, E. M., and Dhe-Paganon, S. (2006) *J. Biol. Chem.* **281,** 38061–38070
34. Hasdemir, B., Murphy, J. E., Cottrell, G. S., and Bunnett, N. W. (2009) *J. Biol. Chem.* **284,** 28453–28466
35. Hislop, J. N., Henry, A. G., Marchese, A., and von Zastrow, M. (2009) *J. Biol. Chem.* **284,** 19361–19370
36. Cao, Z., Wu, X., Yen, L., Sweeney, C., and Carraway, K. L., 3rd. (2007) *Mol. Cell. Biol.* **27,** 2180–2188
37. Wu, X., Yen, L., Irwin, L., Sweeney, C., and Carraway, K. L., 3rd. (2004) *Mol. Cell. Biol.* **24,** 7748–7757
38. Marchese, A., Raiborg, C., Santini, F., Keen, J. H., Stenmark, H., and Benovic, J. L. (2003) *Dev. Cell* **5,** 709–722
39. Hu, C. D., Grinberg, A. V., and Kerppola, T. K. (2005) *Curr. Protoc. Protein Sci.* 19.10.1–19.10.21
40. Nash, P., Tang, X., Orlicky, S., Chen, Q., Gertler, F. B., Mendenhall, M. D., Sicheri, F., Pawson, T., and Tyers, M. (2001) *Nature* **414,** 514–521
41. Bowers, K., Piper, S. C., Edeling, M. A., Gray, S. R., Owen, D. J., Lehner, P. J., and Luzio, J. P. (2006) *J. Biol. Chem.* **281,** 5094–5105
42. Sigismund, S., Woelk, T., Puri, C., Maspero, E., Tacchetti, C., Transidico, P., Di Fiore, P. P., and Polo, S. (2005) *Proc. Natl. Acad. Sci. U.S.A.* **102,** 2760–2765
43. Liu, Q., Berry, D., Nash, P., Pawson, T., McGlade, C. J., and Li, S. S. (2003) *Mol. Cell* **11,** 471–481
44. Lewitzky, M., Harkiolaki, M., Domart, M. C., Jones, E. Y., and Feller, S. M. (2004) *J. Biol. Chem.* **279,** 28724–28732
45. Lewitzky, M., Kardinal, C., Gehring, N. H., Schmidt, E. K., Konkol, B., Eulitz, M., Birchmeier, W., Schaeper, U., and Feller, S. M. (2001) *Oncogene* **20,** 1052–1062
46. Harkiolaki, M., Lewitzky, M., Gilbert, R. J., Jones, E. Y., Bourette, R. P., Mouchiroud, G., Sondermann, H., Moarefi, I., and Feller, S. M. (2003) *EMBO J.* **22,** 2571–2582
47. Scita, G., and Di Fiore, P. P. (2010) *Nature* **463,** 464–473
48. Sierra, M. I., Wright, M. H., and Nash, P. D. (2010) *J. Biol. Chem.* **285,** 13990–14004
49. Mari, M., Bujny, M. V., Zeuschner, D., Geerts, W. J., Griffith, J., Petersen, C. M., Cullen, P. J., Klumperman, J., and Geuze, H. J. (2008) *Traffic* **9,** 380–393
50. Morino, C., Kato, M., Yamamoto, A., Mizuno, E., Hayakawa, A., Komada, M., and Kitamura, N. (2004) *Exp. Cell Res.* **297,** 380–391
51. Lock, L. S., Royal, I., Naujokas, M. A., and Park, M. (2000) *J. Biol. Chem.* **275,** 31536–31545
52. Feng, S., Chen, J. K., Yu, H., Simon, J. A., and Schreiber, S. L. (1994) *Science* **266,** 1241–1247